

Designing 3D gradient coils for open MRI systems

P. T. White¹, L. K. Forbes¹, and S. Crozier²

¹School of Maths and Physics, University of Tasmania, Hobart, TAS, Australia, ²School of Information Technology and Electrical Engineering, University of Queensland, Brisbane, QLD, Australia

Introduction: Traditionally, gradient coil windings are constrained to lie on cylindrical or planar surfaces and their precise locations are found such that they optimise coil properties such as gradient homogeneity, inductance and coil efficiency. To address secondary concerns such as eddy current induction, peripheral nerve stimulation, acoustic noise and overheating, other interesting geometries have been explored (eg [1], [2]). While *et al.* [3] introduce a 3D gradient coil design method in which the precise 3D geometry of the coil windings is found as part of the optimisation. Results display an interesting combination of closed loops and spiral-type windings that lie approximately on the surfaces of sets of elliptical tori. The efficiency and manufacturability of these 3D windings are improved by While *et al.* [4] with the design of toroidal gradient coils of high gradient homogeneity, low inductance, high efficiency and good force balancing, which also offer perceived benefits to gradient cooling and patient claustrophobia. One standard method of reducing patient claustrophobia and improving patient access is to use open biplanar systems [5], however this comes at the cost of lower coil efficiency. Alternative 3D coil windings for this open-type MRI system are explored here using an adaptation to the theoretical 3D gradient coil design method of While *et al.* [3].

Method: For the open 3D system we consider two cylindrical current density volumes of radius 0.5 m, either side of the imaging region, which are concentric with the z -axis. One cylindrical volume extends axially from $z = 0.25$ - 0.35 m and the second volume is symmetric to the first about $z = 0$. A 50 mT/m x -gradient target field is considered within a 0.36 m DSV centred at the origin. Two circular shielding target regions can be included of radius 0.55 m and centred at $z = 0.4$ m and $z = -0.4$ m. The two volumetric current densities are represented using Fourier series in cylindrical coordinates and must be divergence free. The Fourier coefficients are obtained by minimising the field error and a power constraint using a Tikhonov regularisation method similar to [5]; however, the mathematics is greatly complicated by the additional axial coordinate and current density component present in the 3D representation. In addition, the 3D current density can no longer be related to a single streamfunction as for the 2D problem and therefore the convenience of contouring such a streamfunction to obtain coil windings is no longer available. Instead, a priority streamline seeding technique, originally used for mapping velocity fields in fluid flow [6], is adapted to find coil windings which approximate the 3D current density. In this method, streamlines are seeded at the locations of maxima of a density map related to the current density magnitude. A 3D Gaussian filter is then traced along each streamline and the process is repeated to successively lower the density map until some threshold is obtained. Symmetry arguments aid this process greatly.

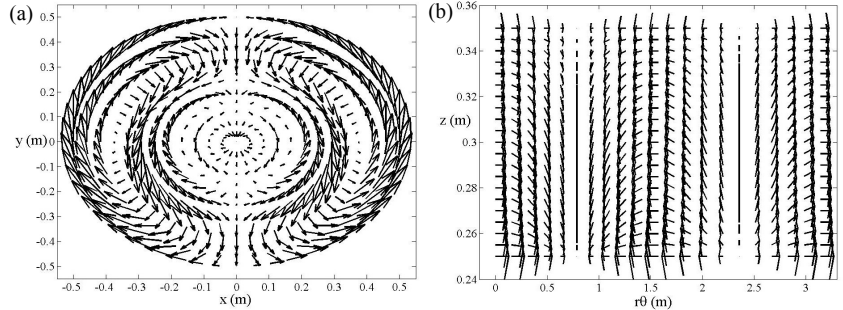


Fig. 1: Unshielded 3D current density: (a) (x,y) plane at $z = 0.25$ m; (b) (r,θ,z) plane at $r = 0.5$ m.

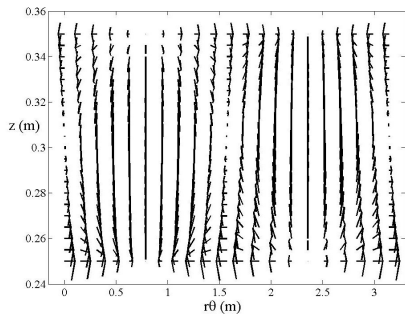


Fig. 3: Shielded case: (r,θ,z) plane at $r = 0.5$ m.

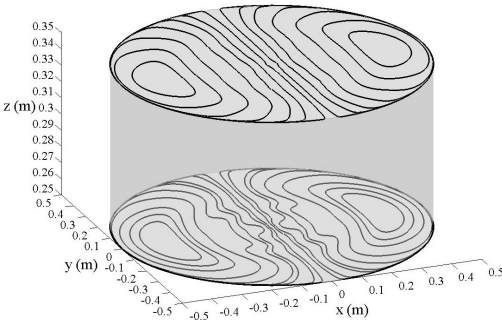


Fig. 4: 3D coil windings for shielded open gradient coil.

Results: The optimisation method allows a trade-off between current density simplicity, field homogeneity and level of shielding. Fig. 1 displays quiver plots on 2D cross-sections of an unshielded 3D current density example, which induces a field with 0.16% field error within the DSV. In Fig. 1(a) the quiver plot is on the surface nearest the DSV of the first coil volume, ie at constant $z = 0.25$ m. Here we note that the current follows crescent-shaped paths on this surface and similar general flow is observed on other cross-sections of constant z . Fig. 1(b) shows the current density on the outer (r,θ,z) plane at constant radius $r = 0.5$ m with apparent sources and sinks representing the flow of current from and to other regions of the coil volume. Fig. 2 displays the result of applying the priority streamline seeding technique to this interesting unshielded 3D current density example. Here we note a concentration of coil windings on the surface $z = 0.25$ m, which are clearly used to induce the gradient field within the DSV, and looped return path windings occurring away from this region. There also exists an interesting feature near the coil centre where the windings are also taken away from $z = 0.25$ m. Figs. 3-4 display similar plots for a shielded 3D current density example, for which the field on the exterior shielding target regions is lower by a factor of 10, at the expense of a slightly elevated field error of 0.22% and increased coil power. A crescent-shaped flow of current is found to occur on the surface $z = 0.25$ m similar to that displayed in Fig. 1(a); however, for cross-sections near the outer surface at $z = 0.35$ m the direction of this current is reversed for the shielded case. This feature is also demonstrated in Fig. 3, which displays the flow of current on the (r,θ,z) plane at constant radius $r = 0.5$ m, and this reversal is perhaps expected for coils with active shielding. Fig. 4 displays the result of applying the priority streamline seeding technique to the shielded example, and here we find that coil windings occur exclusively on the inner and outer surfaces at $z = 0.25$ m and $z = 0.35$ m, respectively. This is interesting as it suggests that the existing biplanar designs for shielded open systems are already optimum, at least with regards to minimising coil power.

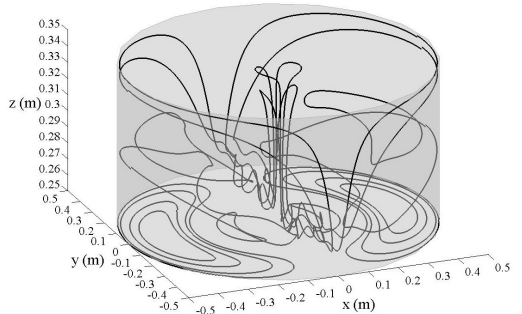


Fig. 2: 3D coil windings for unshielded open gradient coil.

Conclusion: A method has been presented for obtaining theoretically 3D gradient coil windings for an open MRI system. Preliminary results display interesting looped behaviour for an unshielded example and a biplanar form for a shielded example. Further work will include searching for simpler geometries for the unshielded result and comparing coil performance, as well as considering an alternative current density representation for the shielded system to find 3D coil windings within the coil volume. In addition, other geometries may be explored using the 3D design method by optimising coil properties other than power.

- References:** [1] H. Sanchez *et al.*, *IEEE Trans. Magn.*, vol. 43(9), pp. 3558-3566, 2007. [4] P.T. White *et al.*, *J. Magn. Reson.*, vol. 198, pp. 31-40, 2009.
 [2] P. Mansfield & B. Haywood, *Phys. Med. Biol.*, vol. 53(7), pp. 1811-1827, 2008. [5] L.K. Forbes *et al.*, *IEEE Trans. Magn.*, vol. 41(6), pp. 2134-2144, 2005.
 [3] P.T. White *et al.*, *IEEE Trans. Biomed. Eng.*, vol. 56(4), pp. 1169-1183, 2009. [6] M. Schlemmer *et al.*, *Eurographics/IEEE-VGTC Symp. Vis.*, pp. 1-8, 2007.